Available online at www.sciencedirect.com
SCIENCE DIRECT
ELSEVIER
Nuclear Instruments and Methods in Physics Research A 546 (2005) 274–280
NUCLEAR INSTRUMENTS & METHODS IN PHYSICS RESEARCH Section A
www.elsevier.com/locate/nima

Tests of a backside illuminated monolithic CMOS pixel sensor in an HPD set-up ☆

Wojciech Dulinski[a,*], Andrea Braem[b], Massimo Caccia[c], Gilles Claus[a], Grzegorz Deptuch[a], Damien Grandjean[d], Christian Joram[b], Jacques Séguinot[b], Marc Winter[d]

[a] *LEPSI, IN2P3/ULP, 23, rue de Loess, BP20, F-67037 Strasbourg, France*
[b] *CERN, PH Division, CH-1211 Geneve 23, Switzerland*
[c] *Universita degli Studi dell' Insubria, Como, Italy*
[d] *IReS, IN2P3/ULP, 23, rue de Loess, BP20, F-67037 Strasbourg, France*

Available online 19 April 2005

Abstract

A backside illuminated, monolithic CMOS pixel sensor for direct detection of low energy electrons has been developed and is proposed as an active element for a non-destructive hadron beam monitor. In this application, the device is used as an imager of secondary electrons emitted from an aluminium foil of sub-micrometer thick intersecting the beam and accelerated in an electrostatic field to ~20–30 keV energy. The sensitivity to these electron energies (a few microns range in silicon) is obtained by back-thinning the detector, fabricated in the form of standard VLSI chip, down to the radiation sensitive epitaxial layer. The original thinning procedure was applied for processing of a large area, one million pixels prototype. The prototype has been tested using low-energy electrons inside an HPD structure. Tests results proving the device imaging capabilities of such a radiation are presented.

Keywords: Monolithic active pixel sensors; CMOS; Backside illuminated; Low energy electrons detection; HPD

1. Introduction

A Monolithic Active Pixel Sensor (MAPS) integrates on the same substrate the detector element with the processing electronics. The device is fabricated in a standard CMOS process available through many commercial microelectronics companies. The idea of using MAPS for the detection of ionizing radiation, in particular for high-energy charged particles tracking, has been proposed by the IReS-LEPSI team in the beginning of 1999. The ability of the monolithic CMOS sensors to provide charged particle tracking has

☆ Work supported under SUCIMA E.C. Contract N. G1RD-CT-2001-00561.
*Corresponding author. Tel.: +33 3 90 24 28 68.
E-mail address: dulinski@lepsi.in2p3.fr (W. Dulinski).

0168-9002/$ - see front matter
doi:10.1016/j.nima.2005.03.116

been demonstrated on a series of Minimum Ionizing MOS Active sensor (MIMOSA) chip prototypes [1–5]. The development of a backside illuminated MAPS device was done within the framework of the SUCIMA FP5 European Project [6]. One of two tasks of the collaboration is the development of a non-destructive beam monitoring in a hadron-therapy centre. This requires a direct imaging of secondary emission electrons emitted from a sub-micrometer thick Al foil intersecting the beam and accelerated in electrostatic field up to an energy of around 30 keV, corresponding to a few micrometers range in silicon [7]. In order to adapt a standard MAPS device for efficient detection of such electrons, the thickness of the passive entrance window of the device must be reduced to much less than 1 μm. This operation is done after the device has been fabricated by a standard CMOS process provider; it is usually executed by another party and therefore is called post-processing.

2. Backside illuminated monolithic CMOS sensor

2.1. Standard MAPS

The key element of the Monolithic CMOS Active Pixel Sensor is the use of an N_well/P_substrate diode to collect through thermal diffusion the charge generated by the impinging particle in the thin, undepleted silicon underneath the readout electronics (Fig. 1). This solution allows 100% fill factor, as required in tracking applications. In a standard MAPS sensor, a thin radiation sensitive volume (~10 μm of high quality epitaxial silicon) is sitting on top of a thick (hundreds of micrometers) low quality silicon substrate simply serving as mechanical support. The front side of the epitaxial layer is covered by a passive material, made of several layers of metal and silicon oxide used for circuit electrical interconnection. This structure is well adapted to the detection of penetrating, high-energy particles, but is not compatible with a short range of low-energy (tens of keV) electrons. The sensitivity to such electrons may be obtained by back-thinning the device down to the epitaxial layer, by removing all

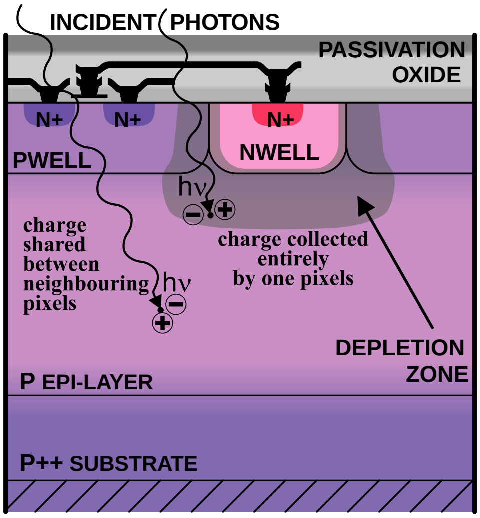

Fig. 1. Cross-section of a silicon wafer showing the principle of a standard CMOS Monolithic Pixel Sensor integrated on the top surface.

of the silicon bulk material. After thinning, the active volume of the detector is directly exposed to the incident radiation. There remains a passive entrance window (mainly silicon oxide for the passivation) with a thickness of the order of 100 nm.

2.2. Post-processing

The back-thinning procedure was developed in collaboration with industry and successfully used for processing of large area ($1.7 \times 1.7\,cm^2$, one million pixels) Mimosa5 MAPS prototypes [8,13]. Before the thinning, the mechanical structure of the chip was reinforced by attaching a several hundreds of microns thick support to the entire front surface. Then the original P++ layer was removed. The exposed surface of epitaxial silicon was passivated, resulting in a thin SiO_2 entrance window. Because of the reinforcing structure, access to the bonding pads of the chip from the original front side was blocked. In order to allow for electrical connections to the chip, a new access path for bonding wires was created from the opposite side, by etching deep trenches in front of bonding pads across the entire thickness of the remaining epitaxial layer (Fig. 2). The

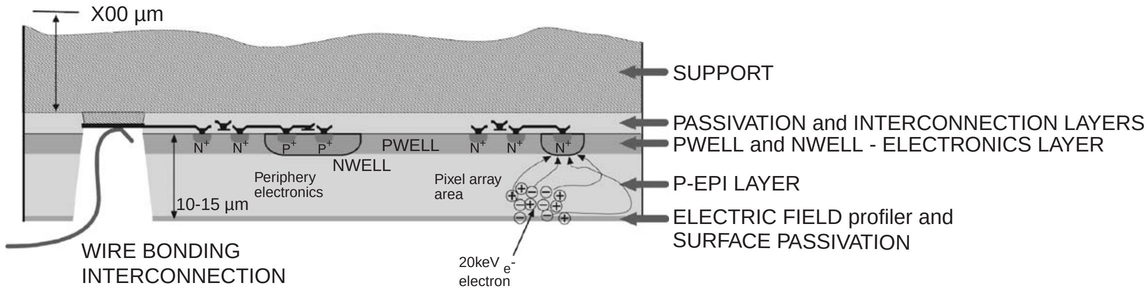

Fig. 2. Cross-section of the back-thinned CMOS monolithic pixel sensor. The low energy electrons impinge on the back (bottom) side of the structure.

post-processing yield was fully satisfactory and several operational chips were obtained. Because of limited area of original bonging metal pads ($90 \times 90\,\mu m^2$), assembly was not trivial and required the use of a 17 µm diameter Al wire and a deep access, fine pitch wedge bonding tool. The chip mounting to the test PCB and following bonding service was provided by a specialized company [9].

2.3. Device calibration using soft X-ray photons

A calibration, performed with a ^{55}Fe 5.9 keV X-ray source, allows to measure the conversion gain and the charge collection characteristics of the device. X-ray photons interact via photoelectric effect inside the active detector volume, and generate an average number of charge carriers of 1640 e/h pairs in silicon. This gives rise to a characteristic peak in the collected charge distribution. For detectors having close to 100% charge collection efficiency, the position of this peak can be directly used for measurements of the conversion gain. This is not the case for the presented device, where the carrier transport mechanism goes mainly through thermal diffusion. Because of a relatively long collection time (in the order of hundred of nanoseconds), some charge losses are therefore expected. The charge is also naturally spread among several pixels. However, the assumption of a fully efficient charge collection is justified for a small sub-sample of photons that convert directly inside the depleted volume of the charge collecting p–n junction. This explains the existence of the small statistics peaks, visible on the right side of the energy spectrum of an individual pixel (Fig. 3, top), in addition to the main peak representing the partially collected charge from photons converted anywhere in the epitaxial volume. The left-side small peak was attributed to the K_α 5.9 keV line and provides the conversion gain. The position of the main peak and its evolution with the number of pixel included in the reconstructed cluster (Fig. 3 middle and bottom) may be used as a tool to estimate the charge collection efficiency from the epitaxial zone. Our previous (still unpublished) measurements with a standard non-thinned Mimosa5 chip shows that 3×3 pixel clusters may account for more than 90% of the charge generated anywhere inside the epitaxial layer.

The basic parameters, like charge-to-voltage conversion factor, noise and leakage current of the thinned devices were found similar to these characterizing non-thinned ones. The total charge collected by a 3×3 pixels cluster amounts for about 60% of the calibration peak value, showing a clear difference with respect to a non-thinned Mimosa5. This may be understood from the particular doping profile close to the $P^{++}_{\text{substrate}}/P^{-}_{\text{epi}}$ and $P^{+}_{\text{well}}/P^{-}_{\text{epi}}$ interface. Such an interface provides a potential barrier high enough to act as a "mirror" for diffusing electrons, keeping them close to the middle of the epitaxial layer and limiting their volume spread. In the process used for Mimosa5 fabrication (AMS 0.6 µm), the initial thickness of the epitaxial layer is 14 µm. However, because of several high temperature processing steps, p-dopant diffusion from the substrate forms a 4 µm thick "transition" layer, where the doping

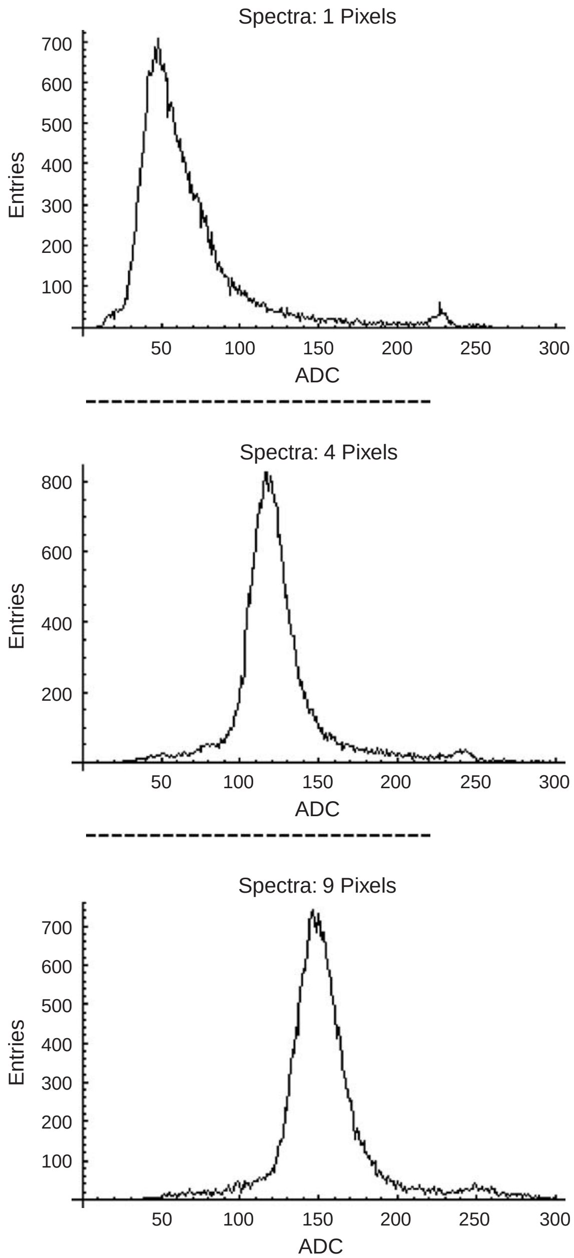

Fig. 3. Collected charge distribution of back-thinned Mimosa5, illuminated with a ^{55}Fe 5.9 keV photons source. Top to bottom: single pixel cluster (central pixel, highest signal), 2×2 and 3×3 clusters.

density decreases smoothly by four orders of magnitude. But, according to microscope inspection of the thinned device edge, this transition layer seems to be entirely etched away, leaving only a 10 μm thick, high resistivity epitaxial layer as active volume. It is therefore possible that such a sharp transition is less efficient as a reflecting layer and part of the charge is lost at the Si/SiO_2 interface. Preliminary results from the beam test [10] show also a substantial decrease of the total charge generated by passing minimum ionising particle, confirming a reduction of the active layer thickness during the back-thinning step.

3. Tests using low energy electrons

3.1. HPD set-up

The used low-energies electrons test set-up contains all basic element of a Hybrid Photon Detectors [11], except for the vacuum tank which is not sealed but connected instead to a pumping system (Fig. 4). The testing of the solid state detector prototype can therefore be done with increased flexibility. A semi-transparent CsI photocathode converts light quanta from a pulsed deuterium filled UV lamp into electrons. These photoelectrons are accelerated by a potential difference between photocathode and a sensor kept at ground potential. A metal plate close to the detector with a circular opening in front of the sensitive area protects the chip periphery (bonding wires) and improves the uniformity of electric field in the central region. During these tests the sensor was kept at room temperature.

According to the electric field simulation (Fig. 5) using the SIMION 3D package [12], the total width of electron position distribution at the detector surface, corresponding to a point-like source at the photocathode, is of the order of 1.5 mm. This is several orders of magnitude more than the expected detector resolution; therefore this electrostatics setting may be used to prove the sensor detection efficiency, but is not appropriate for testing its ultimate spatial resolution.

Back-thinned pixel sensor tests with tunable 5–25 keV mono-energetic electrons were crucial for assessing the feasibility of the beam monitoring system developed within the SUCIMA Collaboration framework.

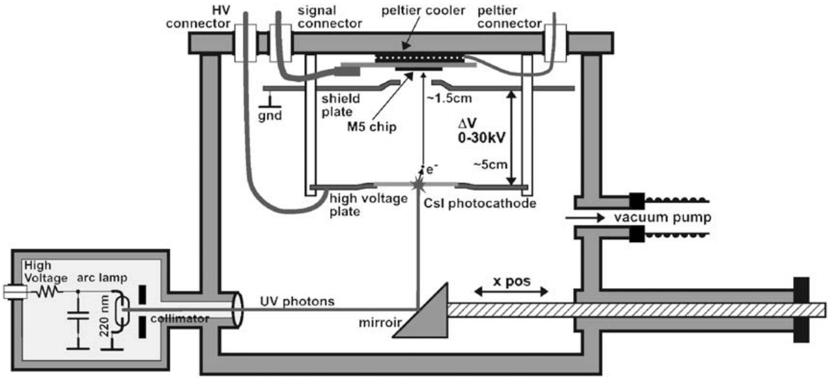

Fig. 4. Schematic of the HPD set-up used at CERN.

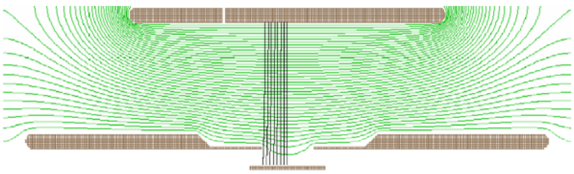

Fig. 5. Simulation (SIMION 3D) of the electric potential distribution and electron trajectories between the CsI photocathode and the Mimosa5 detector.

Fig. 6 shows an overall external and internal view of CERN HPD set-up used for described measurements.

3.2. HPD set-up tests results

Fig. 7 shows typical pulse-high spectra of reconstructed 15 keV electrons, representing the total signal from the central pixel in the cluster (top), cluster of 2×2 pixels (middle) and cluster of 3×3 pixels (bottom). A clear separation of the signal peak from noise is visible.

Fig. 8 shows the measured single electron peak position as a function of the accelerating voltage. In the measured range (from 7.5 up to 20 kV) this dependence is linear. The extrapolated line intercepts the x-axis at 2.48 kV, which may be interpreted as energy loss ($\sim$2.5 keV) in the non-active entrance window. The estimation of the entrance window thickness of this tested detector given by the back-thinning process provider is 160 nm. Detectors

Fig. 6. External (top) and internal view of the HPD set-up at CERN.

with several other window thicknesses (from 75 to 160 nm) were also manufactured and will be tested soon.

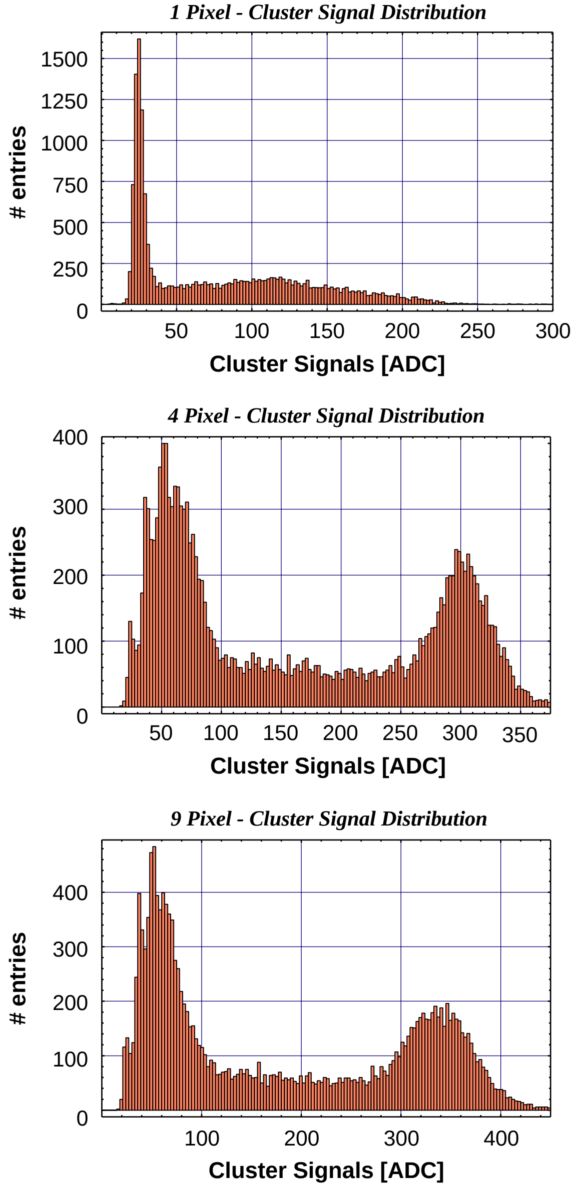

Fig. 7. Collected charge distribution for 15 keV electrons obtained with the back-thinned Mimosa5.

4. Summary and conclusion

An original industrial process was developed and successfully used for back thinning of standard CMOS monolithic pixel sensors down to the epitaxial radiation sensitive layer. The

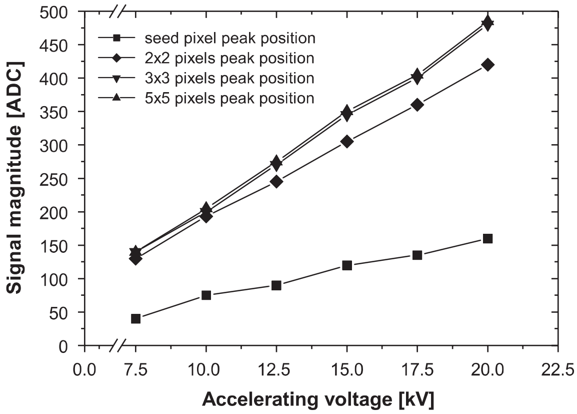

Fig. 8. Total charge amplitude (peak position) of reconstructed hits as a function of accelerating voltage (~electron energy) and cluster size.

ability of a thinned and backside illuminated sensor to efficiently detect electrons in the energy range between 7.5 and 20 keV has been clearly demonstrated. Such a backside illuminated imager may find a number of new applications, in addition to its role as electron imaging device in a non-destructive beam monitor using the SLIM scheme for which it was developed. Some of them, namely autoradiography using a tritium beta source and electron microscopy, have already been explored and results will be published soon [13]. Other applications include thermal neutron imaging with a converter layer deposited directly on the sensor entrance window and single visible light photon imaging using the Hybrid Photon Detector scheme. Still another one which may be considered is sub-micron precision, single particle tracking in proton and ion micro-beam facilities.

Acknowledgments

This work was possible thanks to a continuous support of the SUCIMA team from INP Krakow (Adam Czermak, Barbara Dulny and Bogdan Sowicki) which developed and provided us with the SUCIMA USB DAQ board; a powerful, flexible and easy to use compact data acquisition system [14].

References

[1] R. Turchetta, et al., Nucl. Instr. and Meth. A 458 (2001) 677.
[2] G. Claus, et al., Nucl. Instr. and Meth. A 465 (2001) 120.
[3] G. Deptuch, et al., IEEE Trans. Nucl. Sci. NS-49 (2) (2002) 601.
[4] Yu. Gornushkin, et al., Nucl. Instr. and Meth. A 478 (2002) 311.
[5] G. Deptuch, et al., Nucl. Instr. and Meth. A 511 (2003) 240.
[6] M. Caccia, et al., Nucl. Phys. B (Proc. Suppl.) 125 (2003) 133.
[7] L. Badano, O. Ferrando, M. Pezzetta, G. Molinari, SLIM (sem for low interception monitoring) an innovative non-destructive beam monitor for the extraction lines of a hadrontheraphy centre, in Proceeding of DIPAC, 5–7 May, Mainz, Germany, 2003, pp. 77.
[8] Yu. Gornushkin, et al., Nucl. Instr. and Meth. A 513 (2003) 291.
[9] S.A. Microbonding., rue de l'Areuse 1a, CH 2103 Noiraigue, Switzerland.
[10] A. Besson, Recent progress on Mimosa sensors, presented at the ECFA Meeting, Durham, September 2004, to be published.
[11] C. Joram, Nucl. Phys. B (Proc. Suppl.) 78 (1999) 407.
[12] SIMION 3D Ion Source Software. http://www.srv.net/klack/simion.htm.
[13] G. Deptuch, Tritium autoradiography with thinned and back-side illuminated monolithic active pixel sensor device, preprint LEPSI-2004, Nucl. Instr. and Meth. A 543 (2005) 537.
[14] A. Czermak, et al., Data acquisition system for silicon ultra fast cameras, in: Proceedings of the Seventh International Conference on Advanced Technology and Particle Physics, Villa Olmo, Como, 15–19 October 2001.